ACHIEVING CARBON ECONOMY THROUGH RENEWABLE SOURCES FOR SYNTHESIS GAS

A Thesis

by

HAOYANG LI

Submitted to the Office of Graduate and Professional Studies of
Texas A&M University
in partial fulfillment of the requirements for the degree of

MASTER OF SCIENCE

Chair of Committee,	Mahmoud M. El-Halwagi
Committee Members,	M. Sam Mannan
	Hisham A. Nasr-El-Din
Head of Department,	Muhammad N Karim

May 2017

Major Subject: Chemical Engineering

ABSTRACT

Synthesis gas, known as syngas, is a mixture of hydrogen and carbon monoxide along with other gases. Syngas is an important feedstock for the production of various chemicals and fuels such as ammonia, methanol, dimethyl ether, and Fischer-Tropsch (F-T) liquid fuels. Typically, syngas is produced from the reforming of natural gas. Several mature processes, such as steam methane reforming (SMR), partial oxidation (POX), dry reforming of methane (DR) and autothermal reforming (ATR), are used to produce syngas. A promising alternative to natural gas is biogas (mostly methane and carbon dioxide) which may be used as a feedstock for syngas production. There are some advantages of using biogas as the feedstock: (1) Biogas is considered to be a renewable energy source, which can be produced from several sources of biomass wastes, and (2) Biogas can reduce greenhouse effect by utilizing CO_2 generated from the waste material gasification process and by mitigating the emission of methane.

In order to investigate the economic viability in using biogas for syngas production, fixed and operating cost issues as well as environmental impact must be considered and compared with the use of natural gas.

The thesis investigates the use of biogas for the production of syngas. The separation and reforming units are modeled. The extent of carbon dioxide and methane utilization is assessed. Carbon footprint is included in the objective function. A case study for producing syngas with a ratio $H_2/CO=1.5$ is analyzed and a sensitivity analysis on natural gas price is evaluated to show the feasibility of using biogas instead of natural

gas. The final result shows that in the recent past 20 years, 1/4 of the time favors biogas over natural gas as the feedstock. In other words, biogas is a suitable substitution for natural gas, especially when the natural gas price is higher than about $6.3/MMBtu.

DEDICATION

To my parents

To my girlfriend, Lin Gou

To my friends

With love and gratitude

ACKNOWLEDGEMENTS

I would like to thank my academic advisor, Dr. El-Halwagi, for his constant support and encouragement during my graduate study. I will never forget the smile he always wears on his face. Also I am grateful to my committee members, Dr. Mannan and Dr. Nasr-El-Din, for their support and guidance for my research.

I acknowledge and thank my lab mates and friends in Aggieland for their help and inspiration.

I am truly indebted to my parents for being a permanent source of love. I feel so sorry for not accompanying them these years. I would also like to give my appreciation to my grandfather in heaven. Finally, I express my deepest gratitude to my girlfriend, my future wife, Miss. Lin Gou, for her unconditional love and support.

CONTRIBUTORS AND FUNDING SOURCES

Contributors

This work was supervised by a thesis committee consisting of Professor Mahmoud M. El-Halwagi and M. Sam Mannan of the Department of Chemical Engineering and Professor Hisham A. Nasr-El-Din of the Department of Petroleum Engineering.

The data and figures of TEG absorption dehydration was provided by Professor Bahadori. The model for carbon capture units depicted in Chapter 2 were conducted in part by Professor M.M. Faruque Hasan of the Department of Chemical Engineering.

All other work conducted for the thesis was completed by the student independently.

Funding Sources

There are no outside funding contributions to acknowledge related to the research and compilation of this document.

NOMENCLATURE

F-T	Fischer-Tropsch
SMR	Steam Methane Reforming
POX	Partial Oxidation
DR	Dry Reforming
ATR	Auto- Thermal Reforming
CAGR	Compound Annual Growth Rate
IFA	International Fertilizer Industry Association
CTL	Coal to Liquid
GTL	Gas to Liquid
DOE	Department of Energy
EIA	Energy Information Administration
GHG	Green House Gas
RWGSR	Reverse Water Gas Shift Reaction
MINLP	Mixed Integer Non-Linear Programming
TEG	Triethylene Glycol
TIC	Total Investment Cost
AOC	Annual Operation Cost
TAC	Total Annual Cost
PVAm/PVA	Polyvinylamine/Polyvinylalcohol
IC	Investment Cost

OC	Operation Cost
PSA	Pressure Swing Absorption
VSA	Vacuum Swing Absorption
MEA	Monoethanolamine
PFR	Plug Flow Reactor
RT	Resident Time

TABLE OF CONTENTS

LIST OF FIGURES

LIST OF TABLES

1. INTRODUCTION

1.1 Background and Motivation

Increasing global demand for fuels, industrial chemicals, electricity, and agricultural goods is an important factor to accelerate growth in syngas market. Downstream products of syngas include methanol, ammonia, urea, acetic acid, liquid hydrocarbons produced from Fischer-Tropsch synthesis, etc. The following table provides some of the downstream chemicals and reactions for them via syngas.

Table 1. Selected Syngas Downstream Products and Reactions

Products	**Reactions**
Methanol	$CO+2H_2 \rightarrow CH_3OH$
Ethylene	$2CO+4H_2 \rightarrow C_2H_4+2H_2O$
Aldehyde	$2CO+3H_2 \rightarrow CH_3CHO+H_2O$
Glycol	$2CO+3H_2 \rightarrow HOCH_2CH_2OH$
Propanoic acid	$3CO+4H_2 \rightarrow CH_3CH_2COOH+H_2O$
Acetic acid	$2CO+2H_2 \rightarrow CH_3COOH$

Additionally, the F-T process can be utilized to convert syngas into a variety of hydrocarbons including alkanes and olefins.

General reactions are as follows:

Alkanes: $(2n + 1)\ H_2 + n\ CO \rightarrow C_nH_{(2n+2)} + n\ H_2O$

Olefins: $2n\ H_2 + n\ CO \rightarrow C_nH_{2n} + n\ H_2O$

where n is generally 10-20 depending on different catalysts.

In cobalt-based F-T catalysts, the dominant reaction is typically [2]

$$CO + 2.15H_2 \rightarrow hydrocarbons + H_2O$$

The H_2/CO ratio is about 2.15 as shown in the reaction. When the catalysts are switched to iron-based catalysts, since there exists a water gas shift reaction, the H_2/CO usage ratio is reduced to about 1.7 in low-temperature F-T process, and to approximately 1.05 in the high-temperature process.

1.1.1 Syngas Downstream Product-- Methanol

By far, the dominant methanol synthesis method is based on the synthesis gas process, which was developed in 1920s. In recent years, global methanol demand has experienced a rapid increase. From late 2013 to late 2015, the demand for methanol grew up to 80 million metric tons. In other words, the compound annual growth rate (CAGR) was about 10.7%. Furthermore, it is expected to see an unprecedented growth between 2015 and 2025 with a 4.8% CAGR. Moreover, China and the U.S. are expected to have the largest need for methanol in the future. The following figure shows the global and regional methanol market trend since 2000.

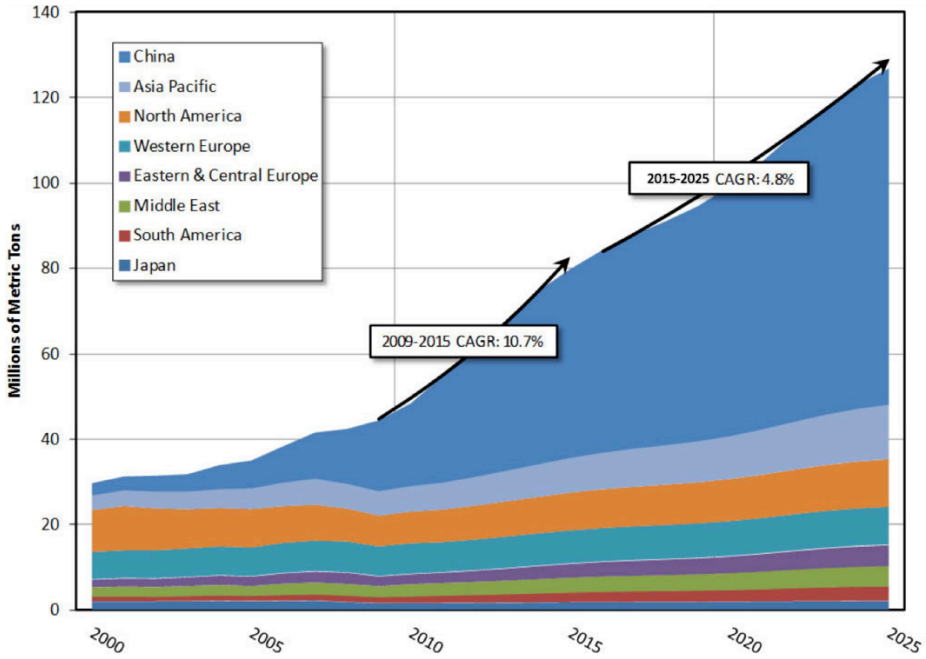

Figure 1. Global and Regional Methanol Market Trend

1.1.2 Syngas Downstream Product-- Ammonia

Another important downstream product of syngas is ammonia. Ammonia is synthesized through the famous Haber process, which follows the reaction shown below, [3]

$$0.5N_2 + 1.5H_2 \rightarrow NH_3 \qquad \Delta H° = -45.7\ kJ/mol$$

Nitrogen can be derived from processed air, which is less expensive and easy to separate. Hydrogen is produced through the syngas production process. First, catalytic steam reforming of methane is used to form hydrogen plus carbon monoxide. [2]

$$CH_4 + H_2O \rightarrow 3H_2 + CO \qquad \Delta H° = 206.2\ kJ/mol$$

The next step is to convert carbon monoxide into carbon dioxide and more hydrogen, which is known as the water-gas-shift reaction. [2]

$$CO + H_2O \rightarrow H_2 + CO_2 \qquad \Delta H° = -41.2\ kJ/mol$$

Over 80% of total produced ammonia is widely used for fertilizing agricultural crops in the world. Based on U.S. Geological Survey, 159 million tons of ammonia was produced in 2010. [4] The International Fertilizer Industry Association (IFA) reported that about 41 million tons of urea capacity are expected to be added between 2013 and 2018. The major increase is in East Asia (15 million tons), Africa (9 million tons) and North America (5 million tons). Figure 2 shows global supplies of ammonia. It indicates that the global demand for ammonia is growing in the next few years. Figure 3 shows regional and sub-regional share of global increase in ammonia from 2014 to 2018. East Asia will potentially have the largest increase in demand for ammonia supplies.

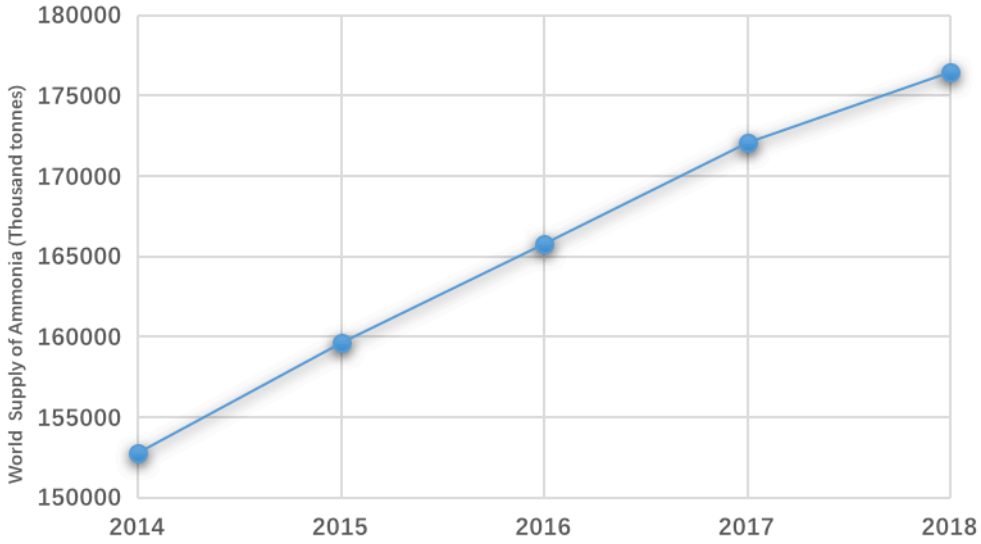

Figure 2. Global Supply of Ammonia, 2014-2018

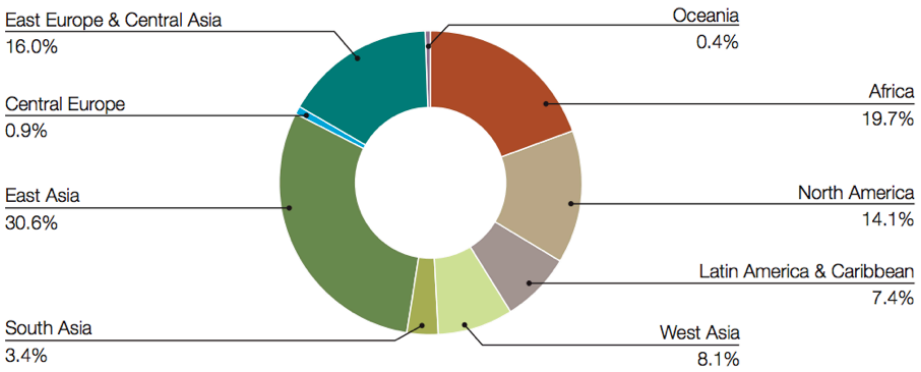

Figure 3. Regional Share of World Increase in Ammonia Supply, 2014-2018. [5]

1.1.3 Syngas Downstream Product-- Liquid Hydrocarbons

In addition to producing methanol and ammonia, syngas could produce liquid hydrocarbons through the F-T process. The F-T process was invented in the 1920s during World War II to supply hydrocarbon fuels for the German war effort. Depending on the source of syngas production, normally coal and natural gas, coal-to-liquid (CTL) and gas-to-liquid (GTL) are two general technologies for the Fischer-Tropsch process. After decades of development, many refinements and adjustments to the technology have been made. Operating plants are using Fischer-Tropsch synthesis all over the world, including Nigeria, Qatar, China, Malaysia, etc. The U.S. Department of Energy (DOE) reported that the most recent facility using the F-T synthesis in the U.S. is Sasol's Lake Charles GTL and Ethane Cracker Complex in Louisiana, which started operating in 2016.

Traditionally, liquid fuels like gasoline and diesel are refined from crude oil. Two other main routes for liquid fuel synthesis are methanol to gasoline and the F-T synthesis. If the oil price remains high, the market demand for CTL and GTL fuel productions would remain high accordingly. However, due to its inherently better

properties, environmental protection, and less separation complexity in liquid fuel synthesis [6], the F-T process is still competitive. Also, with the rapid growth demand of liquid fuels, fuels from the F-T process could potentially have a growing market share around the world, especially in those countries who rely significantly on imported crude oil. Figure 4 illustrates the trend of consumption of petroleum and other liquid fuels from 1990 to 2040 by region. (Data from *International Energy Outlook 2016, EIA*)

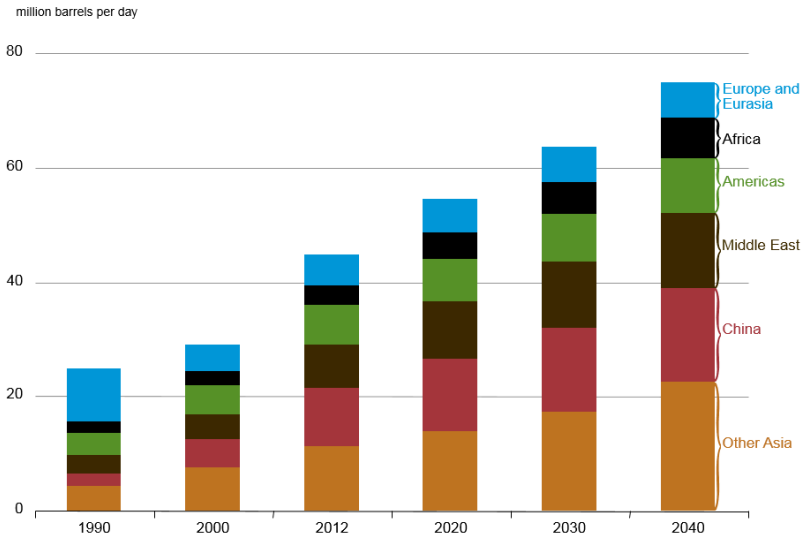

Figure 4. Consumption of Petroleum and Other Liquid Fuels by Region, 1990-2040

According to the above information, three main products from syngas, methanol, ammonia and liquid hydrocarbons through the F-T synthesis, are all experiencing a mushrooming increase, not only in recent years but also in the forecasted period. Furthermore, concerns on environmental protection and increasing initiatives by governments to reduce emissions will spur syngas market growth in the future. Thus, studies on a more economic and more environmentally friendly syngas production process are necessary and pressing.

1.1.4 Syngas Production from Natural Gas

So far, the most economic routes to syngas are natural gas-based processes. [7] Thus, most research and applications largely focus on GTL, and natural gas or shale gas are the most selected feedstocks. However, although natural gas has been regarded as a kind of clean and abundant source, it still has some disadvantages. First, natural gas is non-renewable. While large amounts of natural gas have been discovered over the last decade, experts believe that it will be depleted in the end and this does not meet the requirement for sustainable development. Secondly, natural gas emits some quantities greenhouse gas (GHG), which leads to global warming and climate change. Using natural gas cannot help minimize carbon dioxide emissions. The biggest downside to natural gas is that its lifetime effect of gas mining to the end use, natural gas would cause even larger harm to the environment. In addition to those, even though the price of natural gas exhibits higher stability than the price of crude oil, people cannot guarantee such stability will exist in the long term. According to the data from EIA, in the past 20 years, the natural gas price may range from 1.63$/MMBtu (the lowest) to 6.73$/MMBtu (the highest). The highest recorded value is more than four times the lowest value. Such a fluctuation in resource price will largely affect the investment of a facility and will add uncertainty to the market price.

1.1.5 Syngas Production from Biogas

In order to satisfy the increasing competition, environmental concerns, and societal pressures, a sustainable design, which can maximize the resource utilization and

minimize waste discharge, is crucial. [8] For the syngas production process, people proposed that biogas reforming could be a significant complementary source of syngas, without utilizing fossil fuels in the near future. Also, reactions and catalysts are proven to be effective when using biogas as the feedstock. [9] Several advantages can be seen when using biogas. First, biogas is produced from waste (***e.g.,*** landfill or sewage), so it is considered as a renewable source. It will not be depleted unless humans stop producing waste. Secondly, biogas is non-polluting. Biogas is produced by anaerobic digestion, which is absent of oxygen and no other fuels or energy are needed for converting. Last but not least, it reduces the GHG emission by utilizing gases, which are produced in landfills. Biogas contains mainly methane and carbon dioxide, where carbons are from waste. In other words, carbons may be decomposed into the atmosphere generating greenhouse gas, if not utilized as a form of biogas.

To summarize, biogas has some advantages over natural gas, especially in the sustainable aspect. Therefore, it is worthwhile putting effort to investigate the economic benefit of syngas production using biogas and selecting appropriate reaction route and reaction conditions. Furthermore, considerations on environmental issues are also needed when comparing these two feedstocks.

1.2 Literature Review

Before 21st century, J.R. Rostrup-Nielsen delivered that manufacturing syngas would depend on natural gas and light hydrocarbons for the long term [10]. That is because it will cost more than twice on total investment in building a coal-based plant

than building a natural gas-based plant. Also, natural gas is considered to be the cleanest fossil fuel. Nowadays, natural gas reforming has become a mature process for hydrogen generation. 95% of the hydrogen produced in the U.S. is made by natural gas reforming [11]. Among all the technologies, the most common and economical way to make hydrogen is steam reforming of methane. Two primary reactions can briefly explain how it works.

$$CH_4 + H_2O \rightarrow 3H_2 + CO$$

$$CO + H_2O \rightarrow H_2 + CO_2$$

The first reaction takes place at about 1500 degrees Fahrenheit with nickel catalysts, named as steam reforming reaction. Syngas with H_2/CO ratio of 3 can be produced from this reaction. If additional hydrogen is needed, CO from the reforming reaction may interact with additional steam in the water gas shift reactor, filled with an iron chrome based catalyst (shown in the second reaction).

Partial oxidation of methane (or hydrocarbons) is another pathway for syngas production which is a non-catalytic, large-scale process. This process yields syngas with H_2/CO ratio of about 2 that is optimal for gas to liquid plant [12]. In addition to that, partial oxidation of methane has some other advantages over steam reforming: the selectivity to syngas and the exothermicity. Data regarding CH_4 conversion over different reaction conditions are available through 700K-1200K, 1-20 bar. CH_4/O_2 ratio rises from 1.0 to 5.0 over nickel-based catalysts [13]. Reaction is taken place as following, [14]

$$CH_4 + \tfrac{1}{2}\, O_2 \rightarrow 2H_2 + CO \quad \Delta H_{298K} = -35.6\ kJ/mol$$

Reforming of CH_4 with CO_2, known as the dry reforming of methane, is considered as a promising reaction to mitigate global greenhouse effect by utilizing two main greenhouse gases and producing syngas at the same time. Dry reforming process is more complicated than other two reactions. That is because CO_2 can react not only with CH_4 but also with H_2 simultaneously. This process is known as a reverse water gas shift reaction (RWGSR). Some coke formation reactions will also take place in the dry reforming reactor. Relating reactions are listed below [15].

$$CH_4 + CO_2 \rightarrow 2H_2 + 2CO \qquad \Delta H_{298K} = 246.2\ kJ/mol$$

$$CO_2 + H_2 \rightarrow CO + H_2O \qquad \Delta H_{298K} = 41.4\ kJ/mol$$

$$2CO \rightarrow C + CO_2 \qquad \Delta H_{298K} = -172.4\ kJ/mol$$

$$CH_4 \rightarrow C + 2H_2 \qquad \Delta H_{298K} = 74.9\ kJ/mol$$

$$CO_2 + 2H_2 \rightarrow C + 2H_2O \qquad \Delta H_{298K} = -134.4 kJ/mol$$

By combining non-catalytic partial oxidation and adiabatic steam reforming in a single reactor, auto-thermal reforming is less energy intensive because it uses energy more efficiently than SMR. Reactions with carbon dioxide or steam are described by the following equations.

$$2CH_4 + O_2 + CO_2 \rightarrow 3H_2 + 3CO + H_2O$$

$$4CH_4 + O_2 + 2H_2O \rightarrow 10H_2 + 4CO$$

As shown above, ratios of H_2/CO are 1 and 2.5, respectively. If methane is filled into ATR reactor with oxygen, steam and carbon dioxide, the ratio is varied. Thus, ATR might be another suitable method for syngas production.

Using different processes, such as dry reforming, partial oxidation, steam reforming, and auto-thermal reforming, the syngas ratio varies from 1 to 3. After checking downstream products in Table 1 and other literature, it was found that no matter how the operation condition changes and how the final product varies, nearly all the required ratio for syngas remains 1 to 3. By combining the above routes for syngas generation, it can satisfy the reaction stoichiometry for most downstream chemicals. Among these reactions, dry reforming is a special one because it is indispensable for producing low hydrogen syngas. For example, if the low-temperature F-T process is going to proceed, dry reforming is necessary for a ratio of 1.7 unless we introduce CO additionally. [16] Since it is a CO_2 based reaction, there must be carbon economy behind its application and that is the reason for this research considering the renewable source, biogas, as a feedstock for syngas generation.

1.3 Problem Statement

As mentioned in the previous section, there are several ways for syngas production. Determining the optimal operation condition is essential for each method. Furthermore, if there is a requirement on syngas ratio, which satisfies the downstream operation, what is the best combination of above reforming routes? And what does the term “best” mean? Does that mean most profitable, most environmentally friendly or the combination of these two concerns? In addition to those, this research also focuses on the feasibility of using biogas to take place of natural gas. What is the total cost for a biogas-based facility? Is it cheaper than using natural gas as the feedstock? Since the

natural gas price is changing all the time, what value of the natural gas price will the using of biogas as a substitution be favorable?

To solve these problems, a well-designed superstructure that contains all possible options and a detailed MINLP (mixed integer non-linear programming) model to represent the superstructure are needed. Simulation and optimization software, GAMS and Aspen Plus, are used to help solve these problems.

2. METHODOLOGY

2.1 Superstructure Formation

To conduct a comprehensive evaluation on total syngas generation cost from biogas, three sources of biogas are taken into account. The general sources of biogas are household waste, water treatment plant sludge, and waste of agri-food industry. In this study, the biogas from household waste, water treatment plant sludge, and agrifood industrial waste are represented as biogas 1, biogas 2, and biogas 3, respectively. Compositions of each biogas are listed in Table 2.

Table 2. Compositions of Biogas from Different Sources

Components	**Biogas 1**	**Biogas 2**	**Biogas 3**
CH_4 % Vol	55%	70%	68%
CO_2 % Vol	36%	26%	26%
H_2O % Vol	5%	3%	6%
N_2 % Vol	3%	1%	-
O_2 % Vol	1%	-	-

The overall superstructure is described in Figure 5. In order to help reduce calculation load in GAMS, this problem is divided into two sections: the pre-treatment section and the reforming section. The pre-treatment section includes a dehydration part, a membrane unit and a carbon capture part. As shown in Table 2, all kinds of biogas contain more than 3% of water. However, the membrane in SMR and POX pathways

cannot tolerate water in the feed. SMR and POX pathways are the critical processes to separate carbon dioxide and methane, which are the primary elements in biogas. [17] Membrane is selected to change CH_4 and CO_2 compositions. Moreover, in DR pathway, water is also prohibited because if there is the presence of water, water gas shift reactions are more energetically favored [18]. Thus, a dehydration process is generally conducted at the beginning. After water is removed, biogas containing mainly CH_4 and CO_2 can be sent to DR reformer. Another pathway for dehydrated biogas is entering membrane to adjust CH_4 and CO_2 compositions. Separated CH_4 is used for SMR and POX, and CO_2 is either stored for other use or transferred into DR reformer as CO_2 supplement. If additional CO_2 is required, CO_2 captured from power plant flue gas is another possible carbon dioxide supplement for DR. In the reforming section, syngas from DR, POX and ATR is directly mixed. In SMR pathway, flash unit aims to separated water because water is usually introduced more than methane to increase methane conversion [19]. ATR requires O_2 and H_2O for methane transforming. Therefore, biogas can be directly sent into the ATR reactor for syngas generation. Additional steam is introduced into ATR. The reasons for using steam instead of oxygen are: (1) steam is less expensive than purified oxygen; (2) using steam to reform methane will produce more hydrogen, which is a more useful and higher demand product.

In this study, all the generated syngas is assumed to be well mixed and the syngas ratio of H_2/CO is set to be 1.5. An MINLP model is utilized to simulate the process and to find an optimal solution.

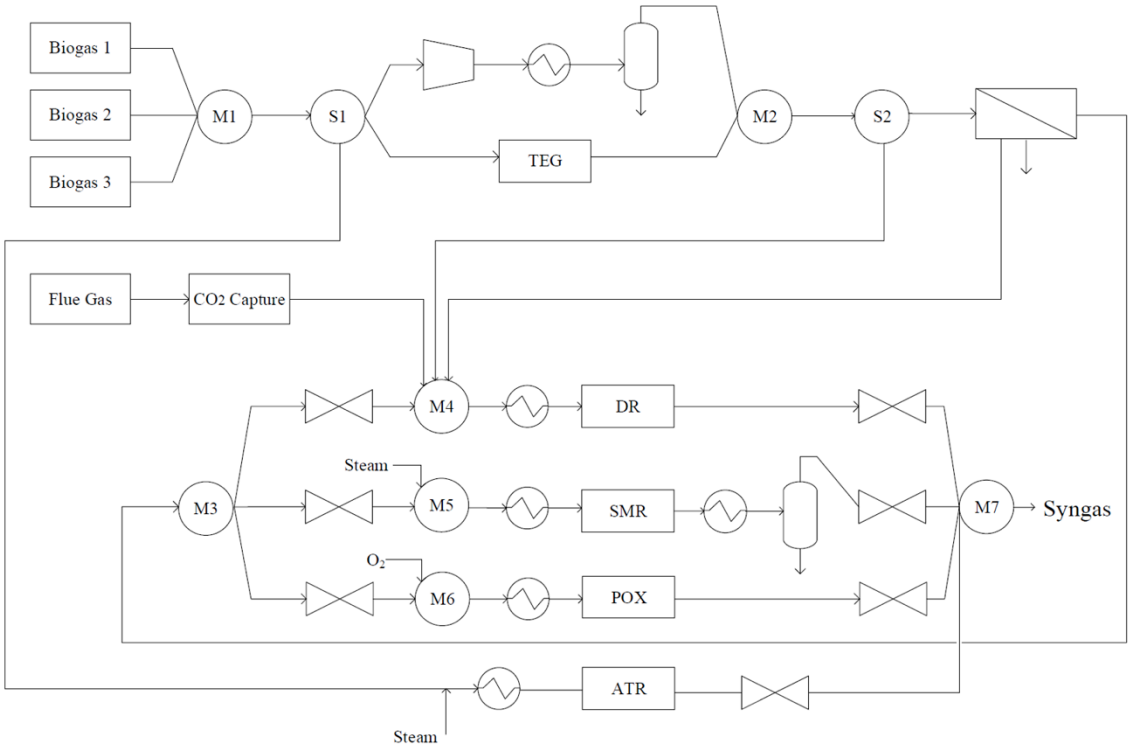

Figure 5. Overall Superstructure for Syngas Production through Biogas

2.2 Pre-treatment Section

Pre-treatment section includes dehydration part, membrane unit and carbon capture part.

2.2.1 Dehydration Part

The Superstructure, model and results will be shown in this chapter.

2.2.2 Superstructure of Dehydration Part

Based on the superstructure shown above, three kinds of biogas should be dehydrated because all of them contain water higher than 3%. Existence of water can

increase the potential risk of corrosion, freezing and hydrate formation in pipes. [20] Condensed water from gas mixture can cause sluggish flowing conditions. Furthermore, water may increase the work load and the heat load due to its high heat capacity. Hence, dehydration of biogas is necessary in this process. Currently, two kinds of equipment are considered in practice. The equipment includes liquid desiccant dehydrator and solid desiccant dehydrator according to the type of the absorbent. Among all the absorbents, glycols are the most popular media because of their properties and commercial application suitability [21]. So far, TEG (Triethylene glycol) is found to be a suitable absorbent because TEG is easily regenerated to a higher degree of purity and its vapor losses is low. Several other processes include refrigeration, compression & cooling are other options for dehydration. In this problem, a basis of biogas flow rate is set to be 1000 mole/s at 1atm, 373.15K. Final water composition is set to be less than 0.1%. A detailed superstructure is provided below.

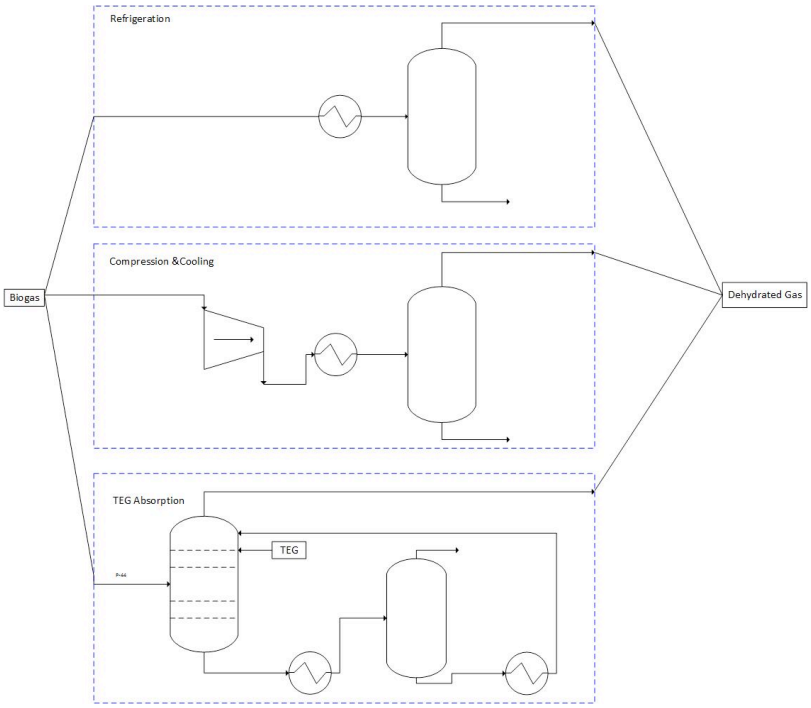

Figure 6. Superstructure for Dehydration Part

In fact, it is not possible to make the water content ratio lower than its saturation composition by just applying refrigeration at 25ºC because of the cryogenic limitations. Simulation from Aspen shows the temperature must drop down to 254.3K, which is below freezing point of water. Thus, only compression & cooling, defined as option 1, and TEG absorption, option 2, are considered in the following model.

2.2.3 Description of MINLP Model of Dehydration Part

The overall cost for dehydration can be calculated with this equation:

$$Total\ annual\ dehydration\ cost = \varphi TIC + AOC$$

where φ is annualizing factor and a value of 0.2 is suggested [22], TIC is total investment cost and AOC is annual operation cost. Expressions for TIC and AOC are given as follows, where y_1 and y_2 represent binary variables. We assume 8000 working hours per year,

$$TIC = C_{cooler}y_1 + C_{compressor}y_1 + C_{Flash1}y_1 + C_{absorber}y_2 + C_{heater}y_2 + C_{cooler}y_2 + C_{Flash2}y_2$$

$$AOC = 8000 * 3600 * (W_{compressor} * Utility\ Cost * y_1 + Q_{cooler} * Cooling\ Utility\ Cost * y_1 + C_{TEG}\ m_{TEG_{MKP}} y_2 + Q_{heater} * Utility\ Cost * y_2 + Q_{cooler} *$$

To begin with, a convex hull formulation is described to guarantee the flow rate can match the binary variable representing that branch.

$$F_0 = F_1 + F_2$$

$$F_1 \leq F_0 * y_1$$

$$F_1 \geq 0$$

$$F_2 \leq F_0 * y_2$$

$$F_2 \geq 0$$

$$y_1 + y_2 = 1$$

In order to reduce the heat load on heater, a compressor is introduced ahead of the heater in option 1. The equation for the compressor is given as followed:

$$W_C = \frac{1}{\eta} F_i T_i R \left(\frac{\gamma}{\gamma - 1}\right) \left(\left(\frac{P_{i+1}}{P_i}\right)^{\left(\frac{\gamma - 1}{\gamma}\right)} - 1 \right)$$

Relation between temperature and pressure is modeled by the ideal gas law:

$$\frac{T_{i+1}}{T_i} = (\frac{P_{i+1}}{P_i})^{(\frac{\gamma - 1}{\gamma})}$$

The performance equations for the heater follows:

$$Q_{heater} = F_i(C_{p_{ave}}(T_i - T_{i+1}) + x_{1_{H_2O}}\Delta H_{vap\_H_2O})$$

where $C_{p_{ave}}$is average heat capacity that is related to composition,

$$\mathrm{C_{p_{ave}}} = \sum_j C_{p_j} x_{i,j}$$

Mass balance, component mass balance and Raoult's law are applied for flash unit:

$$\sum_k F_k = F_i$$

$$\sum_k F_k x_{i,j} = F_i x_{k,i}$$

$$\sum_j x_{k\_j} = 1$$

$$K_{flash,j} x_{k1,j} = x_{k2,j}$$

where $i \in Inlet\ Streams, k \in Outlet\ streams, j \in Components$

The Antione equation for water is given below. The equilibrium coefficients for other components are set to be 10000, which mean little CH_4, CO_2, O_2 and N_2 is transferred into liquid phase:

$$K_{H_2O} = \frac{10\text{^}(A\text{-}\frac{B}{C + T_i})}{P_k}$$

Energy balance is written as:

$$\sum_i F_i T_i C_{p_{ave},i} = \sum_k F_k T_k C_{p_{ave},k}$$

Cost of cooler and compressor can be found in H.P. Loh's process equipment cost estimation report in 2002. [23] The flash drum is regarded as large cylindrical vertical pressure vessels with thickness of 10*mm*. The size and the cost of the vessel are based on the overall vessel weight as shown below:

$$Weight_{flash} = \rho_{steel}\left(\pi\left(H_{flash} + 2th\right)\left(R_{flash} + th\right)^2 \text{-} \pi H_{flash} {R_{flash}}^2\right)$$

Flash unit investment cost follows the following equation: [24]

$$I.C._{unit} = a_{unit} + b_{unit}(S_{unit})^{n_{unit}}$$

Parameters for a, b, n are given in Table 3.

Table 3. Investment Cost Parameters for Typical Equipment [24]

Equipment	**Unit for sizing, S**	**S_lower**	**S_upper**	**a**	**b**	**n**
Flash drum	shell mass, kg	160	250000	11600	34	0.85
Absorber	shell mass, kg	160	250000	11600	34	0.85

Radius can be calculated based on the flow rate. We assume the flash drum with a height to radius aspect ratio of 6:1 [25], and a residence time (*RT*) to be 100 seconds:

$$\pi R_{flash}^2 L_{flash} = 22.4 * F_i{*}RT$$

$$6R_{flash} = H_{flash}$$

Utility cost is collected from U.S. EIA for industrial use in Texas, March 2016 as 5.28 cent/kW·h and cooling utility is estimated by increasing the amount of heat, which must be removed to about 150% [26]. That is because efficiency of energy transferred to

cooling is lower than heating when applying electricity. TEG price is chosen to be $1.54/kg as suggested by ICIS.

When sizing the TEG absorber column, we can calculate the height of it from number of the theoretical stages and the area from mass velocity, G (kg/m^2h), and mass flow rate, m (kg/h), where mass velocity derives from the following equation: [27]

$$G = C_b\sqrt{\rho_V(\rho_L\text{-}\rho_V)}$$

C_b is a coefficient for bubble cap column and ρ_V and ρ_L are vapor density and liquid density, respectively. As shown in Bahadori's work, water removal efficiency (R) is calculated from the following function, where W is the amount of water in the gas:

$$R = (W_{in}\text{-}W_{out})/W_{in}$$

Take biogas from household waste (biogas 1) as an example, the water removal efficiency is 98.1% after calculation with an inlet water composition of 5%. Bahadori [27] summarized the relation among water removal efficiency, TEG circulation rate and TEG purity to different theoretical stages and they are shown in the following graphs.

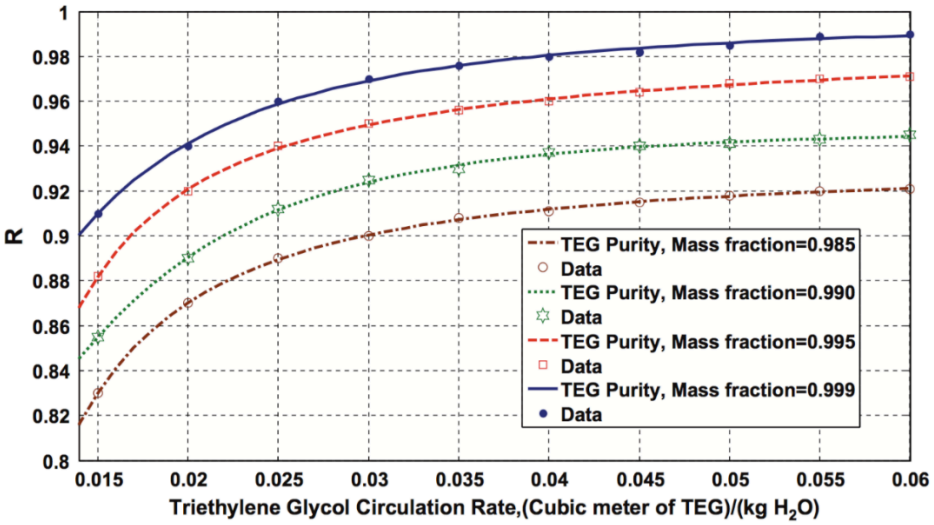

Figure 7. Water Removal Efficiency vs. TEG Circulation Rate at Various TEG Concentrations (Number of Theoretical Stages, N=2.5) in Comparison with Data [28]

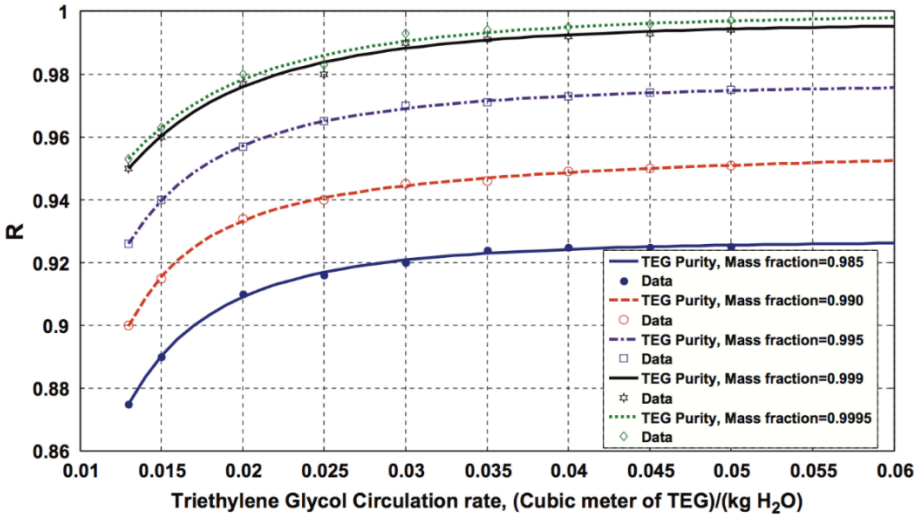

Figure 8. Water Removal Efficiency vs. TEG Circulation Rate at Various TEG Concentrations (Number of Theoretical Stages, N=3) in Comparison with Data [28]

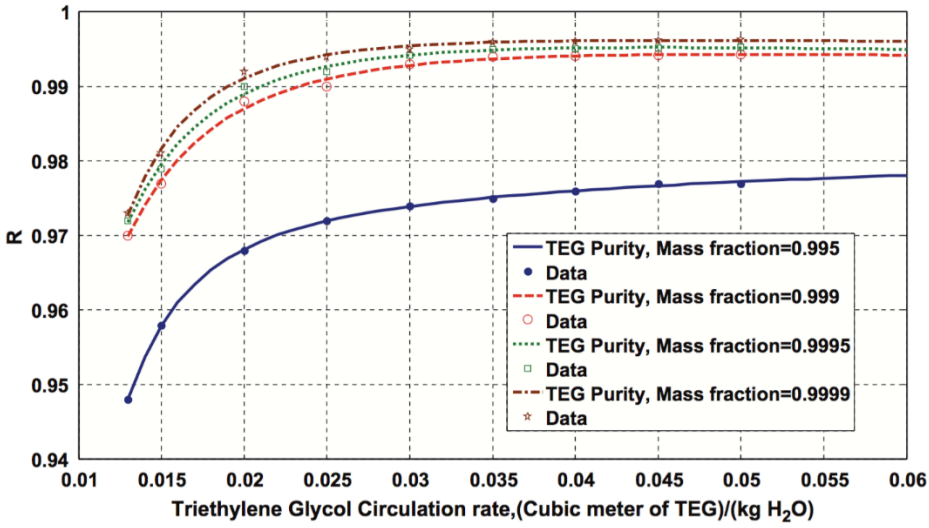

Figure 9. Water Removal Efficiency vs. TEG Circulation Rate at Various TEG Concentrations (Number of Theoretical Stages, N=4) in Comparison with Data [28]

After checking the data in the graphs, the following combinations can satisfy the requirement of 98.1% water removal efficiency. In order to minimize the cost, we choose the lowest TEG circulation rate while satisfying that requirement.

Table 4. Absorber Information to Satisfy Water Removal Efficiency of 98.1%

Theoretical Stage, N_i	**TEG Purity, x_{TEG_i}**	**TEG circulation rate, m_{TEG_i} $(m^3\ TEG/kg\ H_2O)$**
2.5	0.999	0.04
3	0.9995	0.021
3	0.999	0.0225
4	0.9999	0.0145
4	0.9995	0.015
4	0.999	0.016

The height of absorption column can be calculated by applying the following equations:

$$N_{abs} = \sum_i N_i y_{abs\_i}$$

$$H_{abs} = (N_{abs}*4 + 1)*0.6 + 2th$$

where N_i and y_{abs_i} are the number of theoretical stage and the binary variable determining number of stage, respectively.

Two theoretical stages are approximately eight bubble cap trays with 0.6 m tray spacing [26]. The radius of the column is determined by the following equations: [27]

$$A_{in} = \frac{m}{G} = \frac{m}{C_b\sqrt{\rho_V(\rho_L\text{-}\rho_V)}}$$

$$A_{in} = \pi r^2$$

$$A_{out} = \pi R^2 = \pi(r + th)^2$$

where *m* and *G* are mass flow rate and mass velocity, respectively. The weight of the column is given below:

$$Weight_{absorber} = (H_{abs}*A_{out}\text{-}(H_{abs}\text{-}2th)*A_{in} + A_{in}*th * 4 * N_{abs})*\rho_{steel}$$

Investment cost calculation for absorption column follows the same way with flash drum. The corresponding parameters are listed in Table 3. Mass of TEG used in this process (kg/s) can be determined as following:

$$m_{TEG} = \sum_i (x_{TEG_i} * y_{abs_i} * m_{TEG_i}) * \rho_{TEG} * Flow\ Rate_{biogas} * x_{H_2O} * M_{H_2O}/1000$$

where x_{TEG_i} and m_{TEG_i} are obtained from Table 4 and M_{H_2O} is the molecular weight of water. Models for the heater, flash drum and cooler in TEG absorption pathway (option 2) are similar to the previous ones.

2.2.4 Dehydration Part Result

Following results are obtained from simulations in GAMS software.

Table 5. Biogas 1 Dehydrated Result

Biogas 1 (From household waste: 55% CH_4, 36% CO_2, 5% H_2O, 3% N_2, 1% O_2)	
Dehydrated gas flow rate	950.951 mole/s
Dehydrated gas temperature	373.15K
x_{CH_4}	0.5774
x_{CO_2}	0.3786
x_{O_2}	0.0110
x_{N_2}	0.0320
x_{H_2O}	0.0010
Theoretical stages of TEG column	4
TEG Purity	0.9999
TEG circulation rate	0.0145 m^3 TEG/kgH_2O
Cost of absorber	$660,830
Cost of flash drum	$304,870
Overall Cost	$2,566,398.5185

Table 6. Biogas 2 Dehydrated Result

Biogas 2 (From waste water treatment plant :70%CH_4, 26%CO_2, 3%H_2O, 1%N_2)	
Dehydrated gas flow rate	970.971mole/s
Dehydrated gas temperature	373.15K
x_{CH_4}	0.721
x_{CO_2}	0.268
x_{N_2}	0.01
x_{H_2O}	0.001
Theoretical stages of TEG column	4
TEG Purity	0.999
TEG circulation rate	0.012 m^3 TEG/kgH_2O
Cost of absorber	$215,140
Cost of flash drum	$238,110
Overall Cost	$1,343,455.0113

Table 7. Biogas 3 Dehydrated Result

Biogas 3 (From waste of agri-food industry: $68\%CH_4, 26\%CO_2, 6\%H_2O$)	
Dehydrated gas flow rate	940.941 mole/s
Dehydrated gas temperature	373.15K
x_{CH_4}	0.723
x_{CO_2}	0.276
x_{H_2O}	0.001
Theoretical stages of TEG column	4
TEG Purity	0.9999
TEG circulation rate	0.016 m^3 TEG/kgH_2O
Cost of absorber	$233,400
Cost of flash drum	$349,760
Overall Cost	$3,161,626.9827

Comparing to compression & cooling method, using TEG absorption can save 30% of the total cost. The cost for dehydration can be reduced to $3.31/ton, $1.94/ton, $4.69/ton for biogas 1, biogas 2 and biogas 3, respectively.

2.2.5 Membrane Unit

As stated above, purified methane should be supplied to SMR and POX pathways. So in addition to entering DR reformer, dehydrated biogas may also go through a separator which can adjust the CH_4 and CO_2 compositions. Membranes using PVAm/PVA (polyvinylamine/polyvinylalcohol) material are developed. PVAm/PVA membrane ensures high selectivity and CO_2 permeability. Also, this membrane provides long-term stability, excellent mechanical strength and good reproducibility. According to

Deng's work, [29] CH_4 loss in a PVAm/PVA blend membrane is only 0.57%, which is significantly favorable over current commercial membranes. Such a small amount of CH_4 is negligible and we assume the outlet streams are pure CH_4 and CO_2 in retentate and permeant, respectively.

2.2.6 Superstructure of Membrane Unit

Below is the zoom-in superstructure for membrane unit. Since CH_4 and CO_2 in dehydrated biogas reaches up to 95%, dehydrated biogas can partially go straight into DR reactor. Membrane is applied to adjust the composition of the rest of dehydrated biogas so that CH_4 can be separated for feeding SMR and POX reactors. There are two ways to deal with the separated CO_2. DR requires CH_4: CO_2 ratio at 1:1, however, as the results shown in Table 5, Table 6 and Table 7, neither of the biogas has enough CO_2. One of the pathway for separated CO_2 is to enter DR reactor for supplying extra reactant. Because we are not sure if the separated CO_2 is overmuch provided, the other stream is suggested for permeant CO_2. This part of CO_2 may be sequestrated for other use.

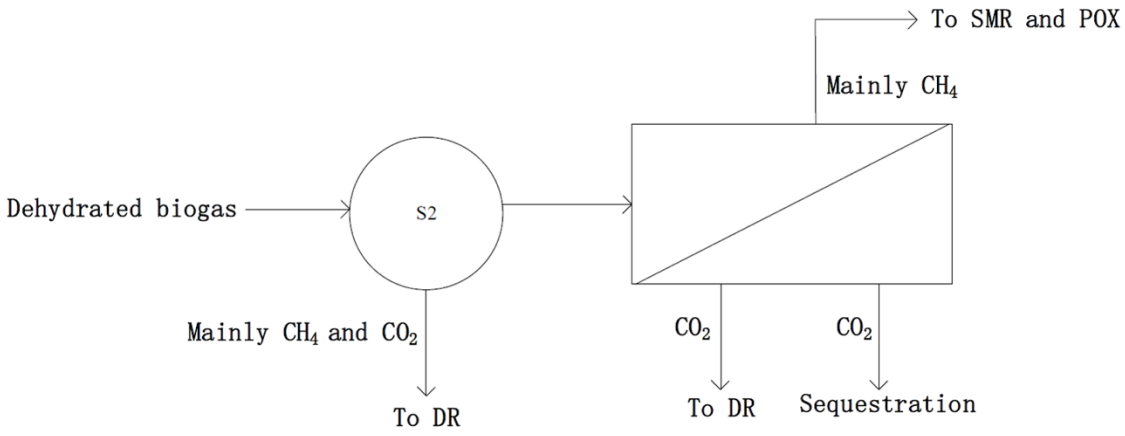

Figure 10. Superstructure for Membrane Unit

2.2.7 Description of Model of Membrane Unit

Hasan developed the investment and operation cost input-output models for several carbon capture technologies based on costs data from rigorous optimization [17]. The following simple expressions for investment cost (IC) and operating cost (OC) are functions of gas flow rate, *F* (mol/s), carbon dioxide composition, x_{CO_2}. Unit for IC and OC is $/yr.

$$IC = \alpha + (\beta x_{CO_2}^{n} + \gamma)F^{m}$$

$$OC = \alpha^{'} + (\beta^{'} x_{CO_2}^{n^{'}} + \gamma^{'})F^{m^{'}}$$

where $\alpha, \beta, \gamma, m, n$ are model parameters and they are listed in Table 8.

Table 8. Parameters for PVAm/PVA Membrane Input-output Cost Model [17]

	α	β	γ	m	n
IC	177500	16505	18912	0.77	0.88
OC	0	11619	0	1	0.21

The flow rate of biogas is determined by the initial set basis. Carbon dioxide composition can be obtained from the previous dehydration part. By combining parameters stated above, cost value can be easily calculated.

2.2.8 Carbon Capture Part

As introduced above, carbon dioxide may not be enough in DR reformer to satisfy the reaction stoichiometry. If DR is more favorable in this situation, there will not be much biogas entering membrane. That means little carbon dioxide from membrane will be supplied into DR. The required CH_4/CO_2 ratio is 1. However, the dehydrated biogas has small amount of carbon dioxide as shown in Table 5, Table 6 and Table 7. Additional CO_2 may be needed for feeding DR. Carbon capture is not necessary if no more CO_2 is needed, but a well-designed superstructure should take into account all possible options.

Power plant flue gas is chosen as the supplement of CO_2 because flue gas is abundant and zero-cost. CO_2 composition of flue gas varies based on different burning fuels: gas-fired flue gas, which contains 7.4-7.7% CO_2, and coal-fired flue gas, which contains 12.5-12.8% CO_2 [30]. These data are useful in evaluating carbon capture cost.

In addition to membrane unit, there are also other carbon capture technologies whose cost can be estimated by previous functions. Actually Hasan provided multiple carbon capture methods with their cost function parameters. In his work, pressure swing absorption (PSA), vacuum swing absorption (VSA), MEA absorption, PZ absorption and membrane are considered. Figure 11 presents total capture and compression cost for each technology regarding different flue gas CO_2 composition.

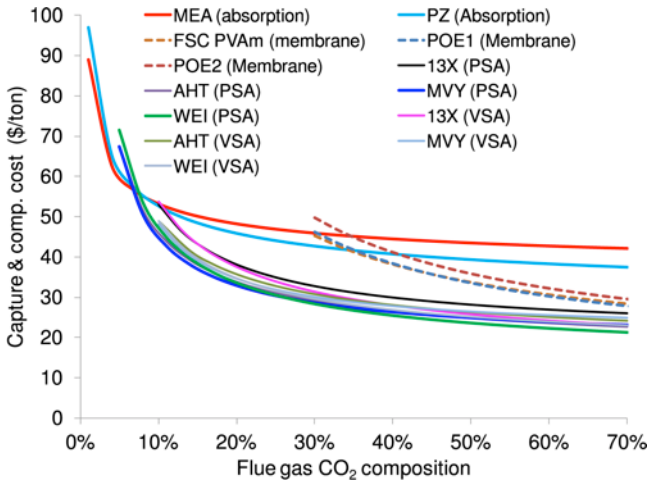

Figure 11. CO_2 Capture and Compression Costs for Various Materials and Technologies[17]

Obviously, MVY-based PSA is a promising and cost-efficient method for capturing carbon from power plant flue gas, where the CO_2 composition is either 7.4-7.7% or 12.5-12.8%. Thus, the model for MVY-based PSA is selected to solve this problem. Values of parameter $\alpha, \beta, \gamma, m, n$ are displayed in Table 9.

Table 9. Parameters for MVY-based PSA Input-output Cost Model [17]

	α	β	γ	m	n
IC	162447	22468	6408.791	0.797	1
OC	0	7265	1839.193	1	1

2.3 Reforming Section

The syngas generation section or reforming section, located at the bottom of figure 5, it is shown below.

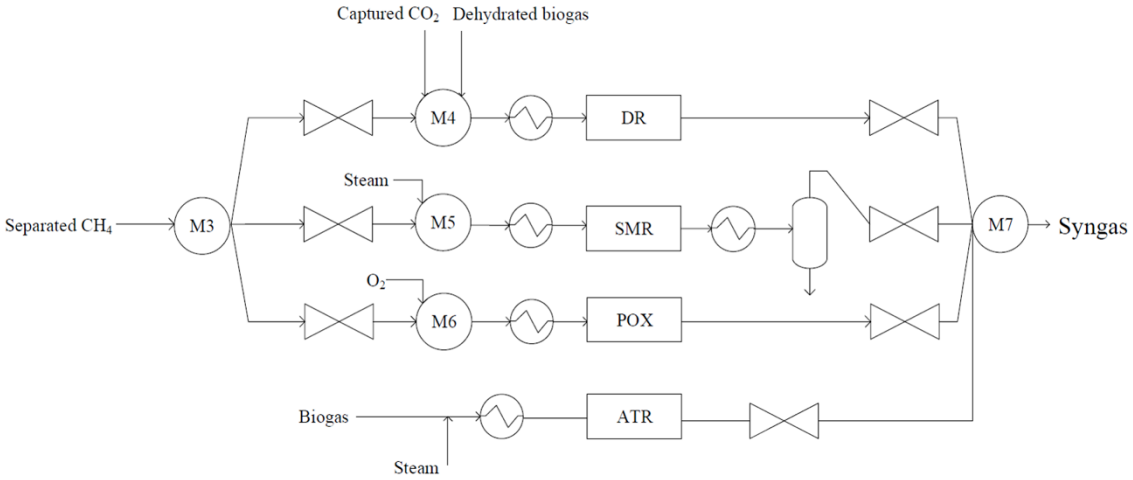

Figure 12. Superstructure for Reforming Section

The input for DR, SMR and POX is the separated CH_4 from previous membrane unit. Methane can go through three different types of reformers to be converted into hydrogen and carbon monoxide. The primary reaction stoichiometry for each reformer and their enthalpies are listed below:

$$CH_4 + CO_2 \rightarrow 2H_2 + 2CO \qquad \Delta H_{298K} = 246.2\ kJ/mol$$

$$CH_4 + H_2O \rightarrow 3H_2 + CO \qquad \Delta H_{298K} = 206\ kJ/mol$$

$$CH_4 + \tfrac{1}{2}\ O_2 \rightarrow 2H_2 + CO \qquad \Delta H_{298K} = -35.6\ kJ/mol$$

ATR requires CH_4, O_2, H_2O and CO_2 as the reactants. These reactants are all involved in biogas. Therefore, biogas can be directly fed as the input into ATR. Since the composition of biogas is fixed and the final syngas ratio is also fixed, the reaction operation condition and the amount of additional steam can be determined by simulation. ATR part is simulated by using Aspen Plus and cost evaluation will be illustrated later.

2.3.1 DR, POX and SMR Part

These reactors are modeled as stoichiometric reactors, which has a variable reaction conversion depending on temperature and pressure. The equation for stoichiometric reactions is shown below:

$$F_k x_{k,j} = F_i x_{i,j} + F_n x_{n,j} + X_{CH_4} \nu_j F_i x_{i,CH_4}$$

where $i\ \epsilon$ inlet stream containing methane, $n\ \epsilon$ other inlet streams, $k\ \epsilon$ outlet streams, $j\ \epsilon$ components, X_{CH_4} refers to CH_4 conversion and ν_j is the stoichiometry of j component. This equation is used to determine how much methane is converted and what is the outlet stream composition after each reforming reaction based on CH_4 conversion. The conversion of methane also determines the heat of reaction equation, which is shown below:

$$Q_l = F_i x_{i,CH_4} X_{CH_4,l} \Delta H_{l,298K}$$

where $l\ \epsilon$ reforming reaction

The next step is to put conversion in terms of pressure and temperature. For each reforming reaction, the graphs are found in the literature which have the relationship between conversion and reaction conditions. A general convex hull formulation is described as:

$$X_l = \sum_s X_s y_s$$

$$T_i = \sum_s T_s$$

$$P_i = \sum_s P_s$$

$$\sum_s y_s = 1$$

$$T_s^{low} y_s \le T_s \le T_s^{high} y_s$$

$$P_s^{low} y_s \le P_s \le P_s^{high} y_s$$

$$X_{\mathrm{s}} = T_s \times slope_{\mathrm{s}} + intercept_{\mathrm{s}}$$

$$slope_{\mathrm{s}} = (X_{T_{\mathrm{s}}^{high}} - X_{T_{\mathrm{s}}^{low}}) / (T_{\mathrm{s}}^{high} - T_{\mathrm{s}}^{low})$$

For the above equations, *s* represents discretized scenarios. The variables for conversion, pressure and temperature, are also discretized. The data obtained under different temperature and pressure is linearly approximated, which is also called linearization. Conversion data and linearization process are shown in the following three figures for DR, SMR and POX. Actually low pressure favors a higher conversion due to the increasing amount of gas molecular in each reaction. And this fact can be discovered in the figures. At the same temperature, conversion under pressure of 1 bar is always higher than conversion under 5 bar, 10 bar and 20 bar. Thus, data at 1 bar is considered in this study. In terms of temperature, it is clear that higher the temperature leads to higher the conversion and this comes to an optimization problem: high conversion

represents more products, which can make more profit but high temperature costs more when operating. To solve this optimization problem, the above MINLP model is created. An example is demonstrated to explain the linearization process.

In Figure 13, conversion at 500℃-600℃, which is the third part of that curve, is a nonlinear expression. Conversion value at 500 ℃ and 600 ℃ are 0.71 and 0.83, respectively. A straight line, whose expression is $X_3 = 0.0012 * T_3 + 0.11$, is used to describe the conversion expression in the range of $T_3^{low} = 500℃$ to $T_3^{high} = 600℃$. Binary variable y_3 is used for indicating if operating condition is selected in this range.

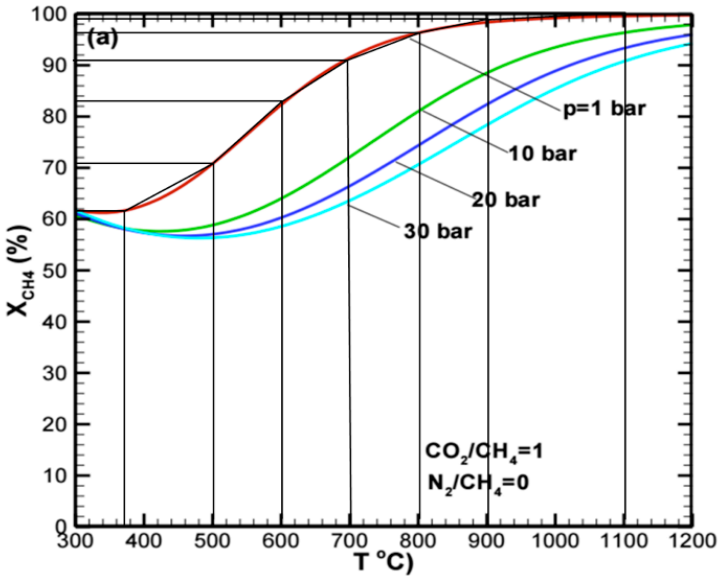

Figure 13. Conversion Linearization for DR Reaction [30]

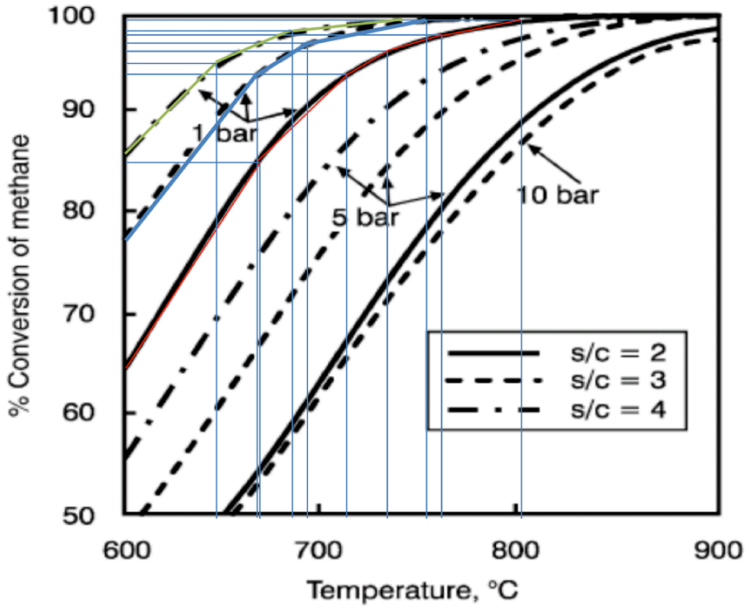

Figure 14. Conversion Linearization for SMR Reaction [31]

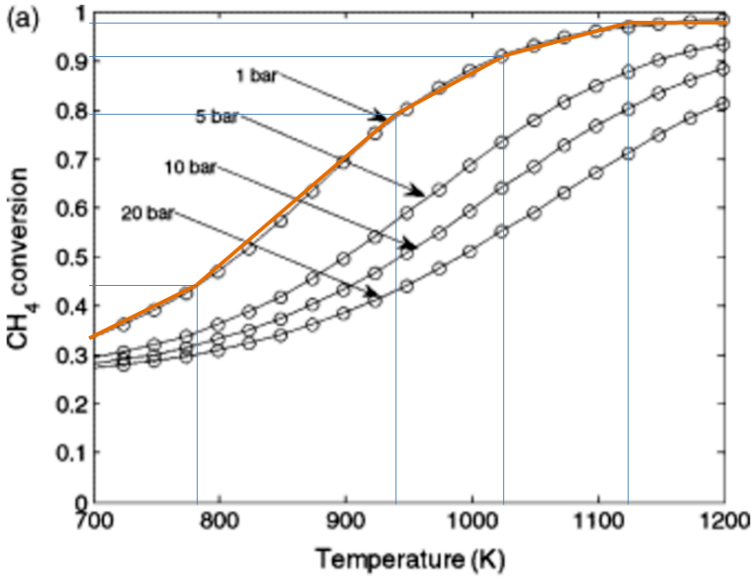

Figure 15. Conversion Linearization for POX Reaction [32]

Once the temperature is determined, heat load of heater ahead of reactor can also be decided by the following equations:

$$Q_{heater,l} = F_i C_{p\_ave} \Delta T$$

$$C_{p\_ave} = \sum_j x_j \, C_{p,j}$$

where $C_{p,j}$ is the heat capacity of component *j*.

The reactor vessels are treated as large cylindrical vertical pressure vessels. The size and the cost are evaluated using the same method as flash unit in the previous dehydration part. The overall weight of the vessel is calculated based on:

$$\pi R_l^2 L_l = F_i * Res\ Time * 22.4$$

$$10R_l = L_l$$

$$Weight_l = \rho_{steel}(\pi L_l((R_l + th)^2 - R_l^2) + 2(th)\pi R_l^2)$$

Reactor length is assumed to be 10 times of the radius to simulate the PFR. Resident time (RT) is supposed to be 100 seconds. *th* represents reactor thickness whose value is presumed as 10*mm*, same as the flash drum. Cost function still follows the equation below whose parameters are listed in Table 10.

$$I.C._{unit} = a_{unit} + b_{unit}(S_{unit})^{n_{unit}}$$

Table 10. Investment Cost Parameters for Reactor Vessel [24]

Equipment	**Unit for sizing, S**	**S_lower**	**S_upper**	**a**	**b**	**n**
Reactor vessel	shell mass, kg	160	250000	11600	34	0.85

Price of O_2 and steam are set to be \$0.021/kg and \$0.006/kg as suggested in paper. [33] [34] Catalysts for SMR and DR are Ni-based and the amount are 2 mol

CH_4/g·h [35] [36]. We assume catalysts are renewed every 6 months and price of Ni-based catalyst is set to be \$100/kg as provided by commercial vendors, such as Alibaba. Annual catalyst cost can be expressed as:

$$C_{cat}(\$/yr) = \frac{3600 F_i x_{i,CH_4}}{2 * 10^3} * 100 * 2$$

So far, models for equipment and their performances have been put forward. TIC includes: PSA, membrane, heaters for three reactions (***e.g.,*** DR, SMR and POX reactors), and cooler and flash drum in SMR pathway. AOC consists: raw materials including biogas, steam and oxygen, OC for PSA, membrane, dehydration, catalyst, and utilities for cooler and heater. Objective function aiming to maximize the profit is defined as:

$$Profit = (mass\ of\ H_2 \times H_2\ price + mass\ of\ CO \times CO\ price)\text{-}TAC$$

Prices of H_2 and CO are \$2/kg and \$0.075/kg, respectively [33]. GAMS software is used for solving the whole model and results will be discussed later comparing to ATR method.

2.3.2 ATR Simulation

The following figure describes the ATR process via biogas.

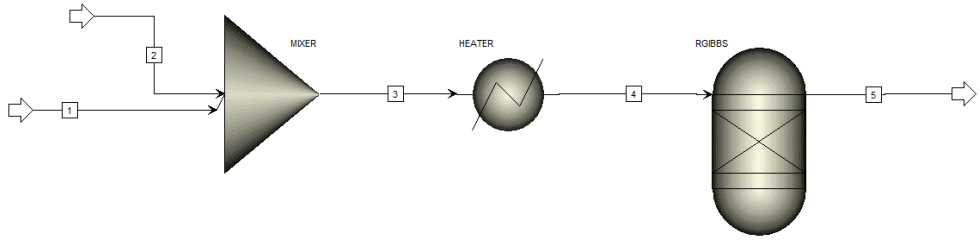

Figure 16. Superstructure for ATR Process

Biogas contains mainly CH_4 and CO_2, and a trace of H_2O and O_2, which are all reactants for ATR. So untreated biogas can be directly sent into ATR reformer. To minimize the free Gibbs energy, an RGIBBS block is chosen. TIC includes heater and reactor. AOC includes raw materials cost, heating utility cost and catalyst cost. Cost of biogas and steam are the same as previous. Utility cost can be calculated when reaction temperature is specified. Amount of catalyst usage also follows the same calculation as last chapter. The composition of input and the product syngas ratio are fixed, and the only parameter which need to be specified is the reaction temperature. In order to find out the optimal reaction temperature for producing syngas with the lowest cost per kilogram, simulation software, Aspen Plus, is applied.

Simulations from 500K to 1300K with the interval of 50K are conducted in Aspen Plus. For each temperature, in order to find out the amount of additional steam for producing syngas with ratio of 1.5, a sensitivity analysis on steam amount is performed. The process is demonstrated by the following example with temperature of 600K.

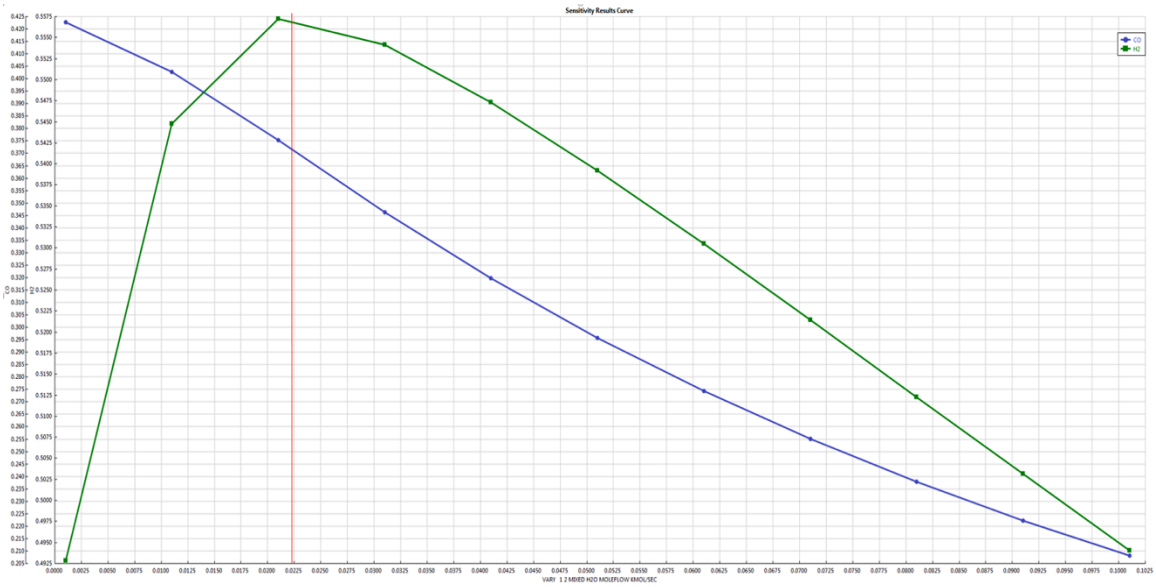

Figure 17. Sensitivity Analysis on Supplied Steam Amount for ATR at 600K

In Figure 17, the green line represents outlet flow rate of H_2 and blue line is the outlet flow rate of CO. With a basis of 100mol/s biogas as the feedstock, when the additional supplied steam is about 22.4mol/s. As shown on the red line, syngas can satisfy the H_2/CO ratio of 1.5 as required. Reenter the steam flow rate of 22.4mol/s for stream 2 and the following results are obtained.

Outlet temperature	600	K
Outlet pressure	100000	N/sqm
Vapor fraction	1	
Heat duty	1.17738e+06	Watt
Net duty	1.17738e+06	Watt
1st liquid / Total liquid		
Pressure-drop correlation parameter		

Figure 18. Heater Simulation Result for ATR at 600K

Outlet temperature	600	K
Outlet pressure	100000	N/sqm
Heat duty	1.23642e+07	Watt
Net heat duty	1.23642e+07	Watt
Vapor fraction	1	
Number of fluid phases	1	
Maximum number of pure solids	0	

Figure 19. Reactor Simulation Result for ATR at 600K

Display Streams Format FULL Stream Table

	5	4	3	2	1	
Substream: MIXED						
Mole Flow kmol/sec						
CH4	0.00148629	0.055	0.055	0	0.055	
CO2	0.0047472	0.036	0.036	0	0.036	
O2	1.26e-21	0.001	0.001	0	0.001	
N2	0.003	0.003	0.003	0	0.003	
H2O	0.00713909	0.0274	0.0274	0.0224	0.005	
CO	0.0847665	0	0	0	0	
H2	0.127288	0	0	0	0	
Total Flow kmol/sec	0.228427	0.1224	0.1224	0.0224	0.1	
Total Flow kg/sec	3.07636	3.07636	3.07636	0.403542	2.67282	
Total Flow cum/sec	11.3953	6.10604	3.79745	0.694958	3.10249	
Temperature K	600	600	373.15	373.15	373.15	
Pressure N/sqm	100000	100000	100000	100000	100000	
Vapor Frac	1	1	1	1	1	
Liquid Frac	0	0	0	0	0	
Solid Frac	0	0	0	0	0	
Enthalpy J/kmol	-4.8207e+07	-1.9098e+08	-2.006e+08	-2.3928e+08	-1.9193e+08	
Enthalpy J/kg	-3.5795e+06	-7.5986e+06	-7.9813e+06	-1.3282e+07	-7.1809e+06	
Enthalpy Watt	-1.1012e+07	-2.3376e+07	-2.4553e+07	-5.36e+06	-1.9193e+07	
Entropy J/kmol-K	60345.4	-7136.41	-27116.2	-36739.7	-28721.4	
Entropy J/kg-K	4480.79	-283.938	-1078.88	-2039.36	-1074.57	
Density kmol/cum	0.0200457	0.0200457	0.0322321	0.0322321	0.0322321	
Density kg/cum	0.269967	0.503823	0.810113	0.580671	0.861508	
Average MW	13.4676	25.1337	25.1337	18.0153	26.7282	
Liq Vol 60F cum/sec	0.0119805	0.00558256	0.00558256	0.00040432	0.00517824	

Figure 20. Stream Simulation Results for ATR at 600K

Follow the same procedures as reforming section, TIC and AOC can be evaluated using the above results from Aspen simulation. Results for ATR simulation and discussion are shown in the next chapter.

3. RESULT AND DISCUSSION

For the ATR pathway, we found the optimal temperature for required syngas with the lowest cost is at 650K. With a 100 mol/s feed biogas 1 basis, total produced syngas is over 61,000 tons annually with a total investment of more than $17 million. Further calculation shows syngas cost per kilogram using biogas 1 is $0.240/kg. For biogas 2 and 3 are $0.286/kg and $0.283/kg, respectively. Thus, on average, using ATR for syngas production from biogas approximately costs $0.27/kg. These are the result after considering carbon economy. For each type of biogas, ATR process can utilize up to 40,000 tons of CO_2 every year and these CO_2 can be quantified with $15/ton as suggested in the report. [37]

If using the combination of DR, SMR and POX, producing the same ratio of syngas costs $3.35/kg, which is much higher than using ATR. Results from GAMS shows the combination of DR and SMR is the most cost-effective combination. Such a high cost is caused from high price of raw material and complicated pre-treatment process.

Price of syngas using natural gas is suggested in Noureldin's work [38]. For the syngas with ratio of 1.5, its cost is $0.261/kg with H_2, which is $2/kg and CO, which is $0.075/kg when natural gas is $3/MMBtu. Compares to $0.27/kg, it seems like using natural gas as the feedstock still costs less than using biogas. However, this value is based on the natural gas price at $3/MMBtu and natural gas price is fluctuating all the time. If natural gas price goes higher, producing syngas with it is bounded to higher cost.

After calculation, when natural gas price is higher than \$6.34/MMBtu, natural gas is no more cost-saving than biogas. Detailed calculation is explained as below.

Syngas with ratio of 1.5 is about \$0.27/kg using biogas based on the calculations in this research. Price of CO is suggested to be \$0.075/kg and this value is considered as a fixed value. Price of H_2 is related to natural gas price. If H_2 price comes to \$2.09/kg, calculated syngas price (\$0.27/kg) will be the same with biogas-based ATR process. Based on the 2013 Energy Outlook report and yearly natural gas price by EIA, we summarize the following table showing price of natural gas and H_2 in different years.

Table. 11 Price of Natural Gas and Hydrogen from 2010 to 2013 [39]

Year	Natural gas price(\$/MMBtu)	H2 price(\$/kg)
2010	4.37	0.9
2011	4.00	0.8
2012	2.75	0.6
2013	3.73	0.7

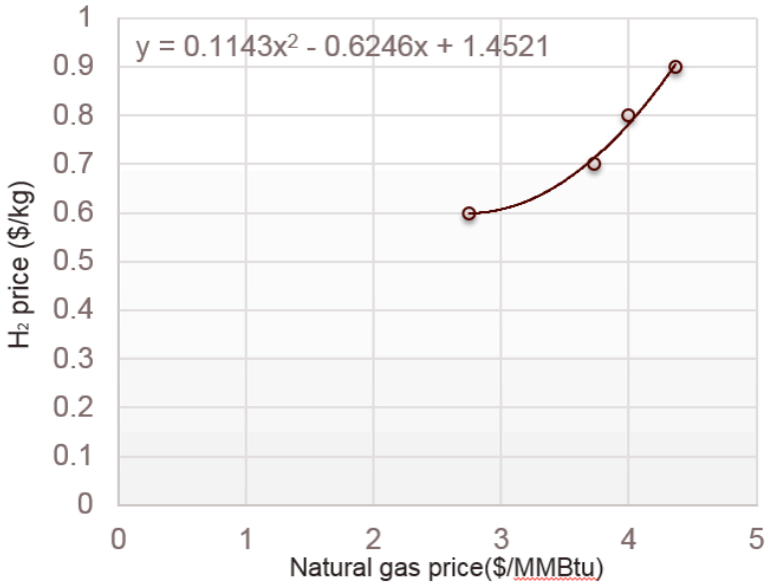

Figure 21. Correlation between Natural Gas Price and Hydrogen Price

Figure 21 shows the correlation between natural gas price and hydrogen price according to the data in Table 11. In the equation shown in the figure, x represents natural gas price and y indicates hydration price. It is easy to solve the x value when y is 2.09, which means hydration price is $2.09/kg. At this point, natural gas price is $6.34/MMBtu.

Figure 22 exhibits the price of natural gas in recent 20 years. The target line of $6.34/MMBtu is displayed (black line). Despite natural gas price is below target line during most of the time, in the year of 2001 and from 2005 to 2009, its value is larger than 6.34 which means using biogas producing syngas costs less than using natural gas in these period.

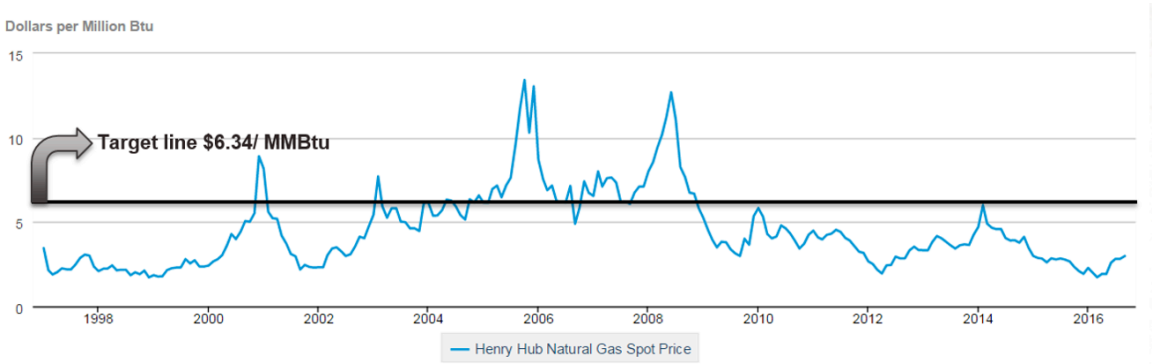

Figure 22. Natural Gas Price in Recent 20 Years

4. SUMMARY

This research provides a techno-economic for syngas production from biogas and compares the results with traditional natural gas-based processes. Several syngas production pathways and pre-treatment units are assessed. The results indicate that biogas usage would have been favored over natural gas in producing syngas for about 1/3 of the past 20 years. The results also show that when natural gas price exceed $6/MMBtu, biogas can potentially expand its market in syngas production.

Nonetheless, there are still existing problems that limit biogas development in industry. These problems include: 1. The relatively limited supply of biogas.; 2. Transportation problems for handling feedstock at large scales. Some supplies (human and agricultural wastes) are not co-located with industrial facilities. Thus, the transportation of raw materials becomes an issue. More energy is needed for the transportation and more CO_2 may be generated during the transportation. 3. High CO_2 content of biogas may offer a challenge to reforming of methane unless substantial separation is used. In order to make biogas widely accepted and applied, solutions and further research for these problems should be provided.

REFERENCES

1. Rathod V, Bhale P V. Experimental Investigation on Biogas Reforming for Syngas Production over an Alumina Based Nickel Catalyst[J]. Energy Procedia, 2014, 54: 236-245.
2. Rostrup-Nielsen J R. Catalytic Steam Reforming[M]/Catalysis. Springer Berlin Heidelberg, 1984: 1-117.3.
3. Modak J M. Haber Process for Ammonia Synthesis[J]. Resonance, 2002, 7(9): 69-77.
4. U.S. Geological Survey, Mineral Commodity Summaries, January 2011
5. Food and Agriculture Organization of the United Nations (2015). World Fertilizer Trends and Outlook to 2018. Retrieved from http://www.fao.org/3/a-i4324e.pdf
6. De Klerk A. Environmentally Friendly Refining: Fischer–Tropsch Versus Crude Oil[J]. Green Chemistry, 2007, 9(6): 560-565.
7. Wilhelm D J, Simbeck D R, Karp A D, et al. Syngas Production for Gas-to-liquids Applications: Technologies, Issues and Outlook[J]. Fuel Processing Technology, 2001, 71(1): 139-148.
8. El-Halwagi, M. M. Chapter 1 - Introduction to Sustainability, Sustainable Design, and Process Integration. In Sustainable Design Through Process Integration; Butterworth-Heinemann: Oxford, 2012; pp 1−14.
9. Domínguez A, Fernández Y, Fidalgo B, et al. Biogas to Syngas by Microwave-assisted Dry Reforming in the Presence of Char[J]. Energy & Fuels, 2007, 21(4): 2066-2071.
10. Rostrup-Nielsen J R. Production of Synthesis Gas[J]. Catalysis Today, 1993, 18(4):

305-324.

11. Hydrogen Production: Natural Gas Reforming, U.S. Department of Energy, Office of Energy Efficiency& Renewable Energy.
12. L.W. ter Haar, J.E. Vogel, in: Proceedings of the Sixth World Petroleum Congress, Frankfurt am Main, Germany, 1963.
13. Enger B C, Lødeng R, Holmen A. A Review of Catalytic Partial Oxidation of Methane to Synthesis Gas with Emphasis on Reaction Mechanisms over Transition Metal Catalysts[J]. Applied Catalysis A: General, 2008, 346(1): 1-27.
14. Song C, Pan W. Tri-reforming of Methane: A Novel Concept for Synthesis of Industrially Useful Synthesis Gas with Desired H_2/CO Ratios Using CO_2 in Flue Gas of Power Plants Without CO_2 Separation [J]. Prepr. Pap.-Am. Chem. Soc., Div. Fuel Chem, 2004, 49(1): 128.
15. Fan M S, Abdullah A Z, Bhatia S. Catalytic Technology for Carbon Dioxide Reforming of Methane to Synthesis Gas[J]. ChemCatChem, 2009, 1(2): 192-208.
16. Dry M E. The Fischer–Tropsch Process: 1950–2000[J]. Catalysis Today, 2002, 71(3): 227-241.
17. Hasan M M F, Boukouvala F, First E L, et al. Nationwide, Regional, and Statewide CO_2 Capture, Utilization, and Sequestration Supply Chain Network Optimization[J]. Industrial & Engineering Chemistry Research, 2014, 53(18): 7489-7506.
18. Buelens L C, Galvita V V, Poelman H, et al. Super-dry Reforming of Methane Intensifies CO_2 Utilization via Le Chatelier's Principle[J]. Science, 2016, 354(6311): 449-452.

19. Oensen F, Rostrup-Nielsen J R. Conversion of Hydrocarbons and Alcohols for Fuel Cells[J]. Journal of Power Sources, 2002, 105(2): 195-201.
20. Gandhidasan P, Al-Farayedhi A A, Al-Mubarak A A. Dehydration of Natural Gas Using Solid Desiccants[J]. Energy, 2001, 26(9): 855-868.
21. Bahadori A, Vuthaluru H B. Explicit Numerical Method for Prediction of Transport Properties of Aqueous Glycol Solutions[J]. Journal of the Energy Institute, 2009, 82(4): 218-222.
22. Towler G, Sinnott R K. Chemical Engineering Design: Principles, Practice and Economics of Plant and Process Design[M]. Elsevier, 2012.
23. Loh H P, Lyons J, White C W. Process Equipment Cost Estimation. Final Report, National Energy Technology Center[J]. 2002.
24. Sinnott R K. Chemical Engineering Design: SI Edition[M]. Elsevier, 2009.
25. STANLEY W, Walas E. Chemical Process Equipment-Selection and Design[J]. Butterman-Heinemam Series, 1990.
26. Alt C. Ullmann's Encyclopedia of Industrial Chemistry[J]. 2006.
27. Bahadori A, Vuthaluru H B. Simple Methodology for Sizing of Absorbers for TEG (triethylene glycol) Gas Dehydration Systems[J]. Energy, 2009, 34(11): 1910-1916.
28. Gas Processors Suppliers Association. GPSA Engineering Data Book. 12th ed. Tulsa, OK: Gas Processors Suppliers Association; 2004. Section 16, p. 1–13.
29. Deng L, Kim T J, Sandru M, et al. PVA/PVAm Blend FSC Membrane for Natural Gas Sweetening[C]/Proceedings of the 1st Annual Gas Processing Symposium. Amsterdam: Elsevier, 2009: 247-255.

30. Chein R Y, Chen Y C, Yu C T, et al. Thermodynamic Analysis of Dry Reforming of CH_4 with CO_2 at High Pressures[J]. Journal of Natural Gas Science and Engineering, 2015, 26: 617-629.
31. Liu J A. Kinetics, Catalysis and Mechanism of Methane Steam Reforming[D]. Worcester Polytechnic Institute, 2006.
32. Enger B C, Lødeng R, Holmen A. A Review of Catalytic Partial Oxidation of Methane to Synthesis Gas with Emphasis on Reaction Mechanisms over Transition Metal Catalysts[J]. Applied Catalysis A: General, 2008, 346(1): 1-27.
33. Noureldin M M B, Elbashir N O, El-Halwagi M M. Optimization and Selection of Reforming Approaches for Syngas Generation from Natural/shale Gas[J]. Industrial & Engineering Chemistry Research, 2013, 53(5): 1841-1855.
34. Kumana J. How to Calculate the True Cost of Steam[R]. DOE/GO-102003-1736. US Department of Energy, Washington, 2003.
35. Liu J A. Kinetics, Catalysis and Mechanism of Methane Steam Reforming[D]. Worcester Polytechnic Institute, 2006.
36. Barroso Quiroga M M, Castro Luna A E. Kinetic Analysis of Rate Data for Dry Reforming of Methane[J]. Industrial & Engineering Chemistry Research, 2007, 46(16): 5265-5270.
37. Brian C. Murray, Christopher S. Galik, and Tibor Vegh. 2014. Biogas in the United States: An Assessment of Market Potential in a Carbon Constrained Future. NI R 14-02. Durham, NC: Duke University.
38. Noureldin M, El- Halwagi M M. Synthesis of C- H- O Symbiosis Networks[J].

AIChE Journal, 2015, 61(4): 1242-1262.

39. Annual Energy Outlook 2013, DOE/EIA-0383, April 2013